

USE OF AN ULTRAHIGH VACUUM BALANCE FOR THE QUANTITATIVE ASSAY OF EVAPORATED  
REFERENCE LAYERS

H.L. ESCHBACH, I.V. MITCHELL and E. LOUWERIX

Commission of the European Community, Joint Research Centre, Central Bureau  
for Nuclear Measurements, Steenweg naar Retie, B-2440 Geel, Belgium

ABSTRACT

The weighing procedure of an ultrahigh vacuum microbalance, which was described previously, has been modified. Examples for various application of the balance will be given. In particular recent use of the microbalance for the definition of areal densities of thin films and self-supporting foils, produced as reference materials for high precision measurements will be discussed.

---

INTRODUCTION

Within the framework of our programme to produce thin boron layers for neutron cross section measurements, a vacuum microbalance has been developed to determine the mass deposited on a quartz disk with high accuracy (ref. 1). An improved design of the first model led to an ultrahigh vacuum compatible concept (ref. 2,3). Although the balance has been designed primarily for the preparation of various standard layers by vacuum evaporation (ref. 4,5), it has also found some different and even non-vacuum applications. The balance has been employed for pressure measurements as a Knudsen type manometer in the  $10^{-5}$  to  $10^{-3}$  mbar region (ref. 6). By measuring changes in buoyancy forces the balance could be used to assay precisely the composition of binary gas mixtures (ref. 7). At atmospheric pressures highly accurate measurements of drop weights of radioactive solutions could be performed (ref. 8).

In the following recent applications of the microbalance to the characterization of thin evaporated reference layers will be discussed. The performance of the balance will be compared with that of other sensitive methods and in particular with the quartz crystal thin film monitor.

## EVAPORATION SYSTEM AND GENERAL FEATURES OF THE MICROBALANCE

The uhv evaporation system used for most of the experiments is an all metal system bakeable to 400°C and pumped by two ion getter pumps to a base pressure of about  $10^{-10}$  mbar. All metal evaporations are performed by electron bombardment from a three crucible source. A resistance heated boat serves for the evaporation of sodium chloride. A schematic diagram of the microbalance is given in Fig. 1.

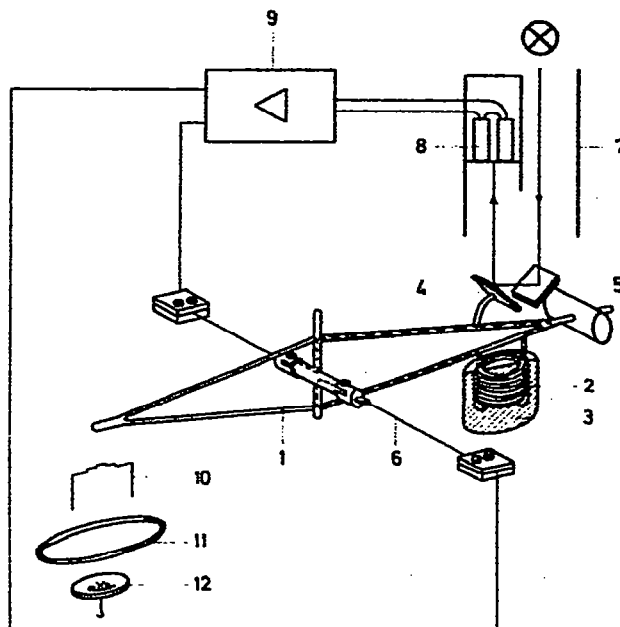


Fig. 1. Schematic diagram of UHV microbalance; 1 balance beam, 2 balance coil, 3 pot magnet, 4 detection mirror, 5 reference mirror, 6 suspension wires, 7 autocollimator, 8 photodiodes, 9 control unit, 10 calibration weight, 11 reference weight, 12 sample pan.

Essentially it is a torsion balance with a beam (1) made of fused silica rod and suspended by two tungsten wires (6) each 40 mm long and 0.1 mm in diameter. At one end of the beam the sample to be measured (12) is suspended. It can be replaced by a reference weight (11). The sample and the reference weight have nearly the same mass, so that at every stage of its operation the balance is under full load. The mass of the deposit is determined as a function of the calibration weight (10), which can be placed together with the sample (12) or with the reference weight (11) on the balance.

The main characteristics of the microbalance are:

- its useful load of 2.5 g with a total weighing range of 20 mg. For special applications (ref. 7) the load could be increased to 10 g.
- a reproducibility of  $< 0.3 \mu\text{g}$  (standard deviation); for the 10 g version the reproducibility was  $1 \mu\text{g}$  in vacuum and  $2 \mu\text{g}$  at atmospheric pressure.

- compatibility with bakeable uhv systems.
- mass determinations by applying the principle of substitution weighing; this eliminates drifts of zero and electrical sensitivity.

#### ABSOLUTE MASS DETERMINATION

The weighing procedure has been simplified by introducing the calibration weight. Fig. 2 shows some details of the load side of the balance beam (B).

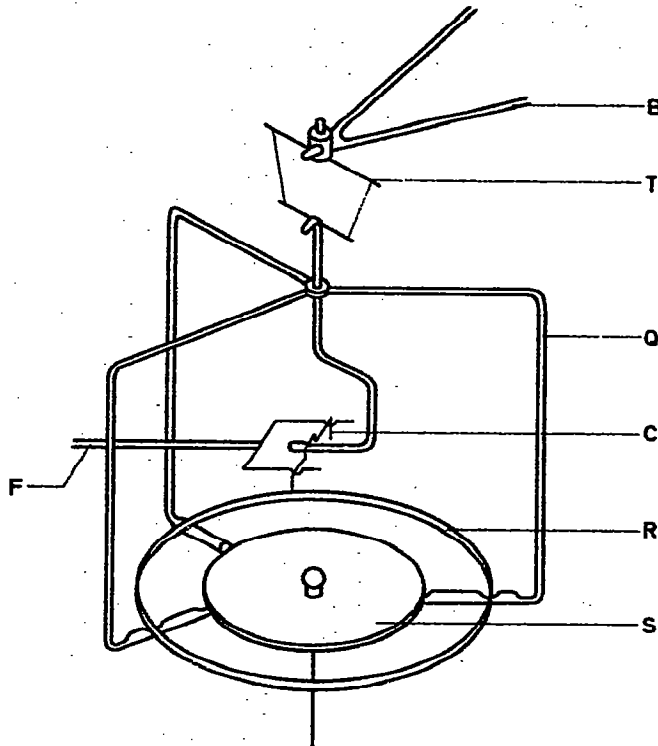


Fig. 2. Quartz carrier with calibration weight.

The pivot point is formed by a triangle (T) with tungsten torsion wires of 0.05 mm diameter. The triangle is fixed to the balance beam by a small screw. The quartz carrier (Q) can be loaded by stainless steel forks (not shown) either with the sample pan (S) or the reference weight (R). In addition the calibration weight (C) can be placed on the carrier.

Let  $c$ ,  $r$  and  $s$  be the mass of the calibration weight, the reference weight and the sample respectively and  $C$ ,  $R$  and  $S$  the corresponding balance readings. Then the following relation holds:

$$s - r = \frac{S - R}{(R+C) - R} \cdot c \quad (1)$$

Let (1) describe a weighing before an evaporation. If we denote by a dash the changed quantities after deposition of a layer, we get:

$$s' - r = \frac{S' - R'}{(R'+C') - R'} \cdot c \quad (1a)$$

The mass  $m$  of the deposit can be calculated from

$$m = s' - s = \left[ \frac{S' - R'}{(R'+C') - R'} - \frac{S - R}{(R+C) - R} \right] \cdot c \quad (2)$$

In general ten independent readings are taken for each measurement and evaluated statistically.

It is evident that the accuracy of the weighing depends directly on the accuracy with which the mass of the calibration weight has been determined and on the stability of this mass. Table 1 lists the mass determinations of a calibration weight used over a period of more than 10 years. The mean of all measurements is  $c = 9423.6 \mu\text{g} \pm 1.5 \mu\text{g}$  ( $n = 13$ ).

TABLE 1

Mass determination of calibration weight

Date of measurement	c [ $\mu\text{g}$ ]	Date of measurement	c [ $\mu\text{g}$ ]
09.07.1970	9423.5	01.10.1971	9423.6
26.10.1970	9424.8	26.10.1971	9421.6
16.12.1970	9424.8	18.11.1971	9421.4
23.03.1971	9424.5	05.04.1972	9422.5
18.05.1971	9424.5	12.01.1978	9424.8
11.08.1971	9421.8	01.08.1980	9426.2
09.09.1971	9422.6		

One of the most important advantages of the microbalance in comparison with other measuring techniques is the direct traceability of the measurements to a primary mass standard. By applying the substitution principle and carefully weighing the calibration weight  $c$ , absolute mass determinations can be performed.

#### COMPARISON OF THE MICROBALANCE WITH A QUARTZ CRYSTAL THIN FILM MONITOR

Taking all possible uncertainties into account, areal densities can be determined with an uncertainty of less than  $0.1 \mu\text{g cm}^{-2}$  when using a microbalance. With quartz crystal monitors, which were first introduced by Sauerbrey (ref. 9), the resolution is  $0.02 \mu\text{g cm}^{-2}$  or better. A direct comparison between microbalance and quartz monitor has been obtained by suspending a quartz and its oscillator from a vacuum balance (ref. 10). With careful shielding good

agreement (within 0.4 %) was found in the case of indium between the mass indication of the microbalance and the quartz monitor. However, the temperature dependence of the frequency of the quartz resonator is a seriously limiting factor (for discussion see e.g. Maissel and Glang (ref. 11)). Recently Ramadan et al. (ref. 12) have shown that in addition to proper shielding, a carefully matched pair of quartz crystals, with respect to their temperature dependence, has to be chosen in order to obtain the highest accuracy and resolution in the mass determination.

For the preparation of reference layers a commercial, water-cooled quartz crystal monitor<sup>†</sup> served as a rate meter. Rate deposition measurements cannot be performed easily using the microbalance and the combination of the two devices is very effective for the production of accurately defined deposits of a definite thickness.

For most evaporations an aluminium disk of 50 mm diameter served as the substrate. To ensure good uniformity in the evaporated layers and to maintain low substrate temperatures a large source to substrate distance of 590 mm was chosen.

At the end of an evaporation cycle the quartz readings for total layer thickness were compared with the balance measurements. A typical set of results is shown in Table 2.

TABLE 2  
Comparison of layer thickness measurements

Material	$M_{\text{Bal}}^{-2}$ [ $\mu\text{g cm}^{-2}$ ]	$M_{\text{Qu}}^{-2}$ [ $\mu\text{g cm}^{-2}$ ]	$\Delta M$ [%]
Au	81.5	81.1	- 0.48
Au	83.5	83.4	- 0.14
Au	49.0	48.9	- 0.28
Au	48.0	48.1	+ 0.12
Al	32.4	32.0	- 1.20
Al	27.4	27.3	- 0.40
Al	54.1	54.1	0
Al	26.6	27.0	+ 1.50
Ni	27.8	27.1	- 2.55
Ni	26.9	27.1	+ 0.74
Cr	72.8	72.7	- 0.14
Cr	71.7	73.1	+ 1.93

From table 2 it can be seen that in general the differences between the two systems are below 2 %, in the case of gold they are smaller than 0.5 %.

<sup>†</sup>Fa Inficon/Leybold-Heraeus.

It is believed that the occasional differences between balance and quartz-monitor are due to the erratic temperature dependence of the resonant frequency as observed by Ramadan et al. (ref. 12).

#### ASSAY OF REFERENCE LAYERS USING A MICROBALANCE

There is an increasing demand for accurately defined thin layers and foils for the calibration of instruments used for the analyses of surfaces and near surface regions. The uhv microbalance has proven to be an extremely useful tool for the characterization of such layers and foils.

#### Layers for RBS analysis

In the past decade, nuclear backscattering of MeV energetic light ions from surfaces (Rutherford backscattering; RBS) has been developed into a technique for rapid, non-destructive and quantitative surface analysis. In essence the RBS technique is straightforward. Fig. 3 illustrates the experimental procedure.

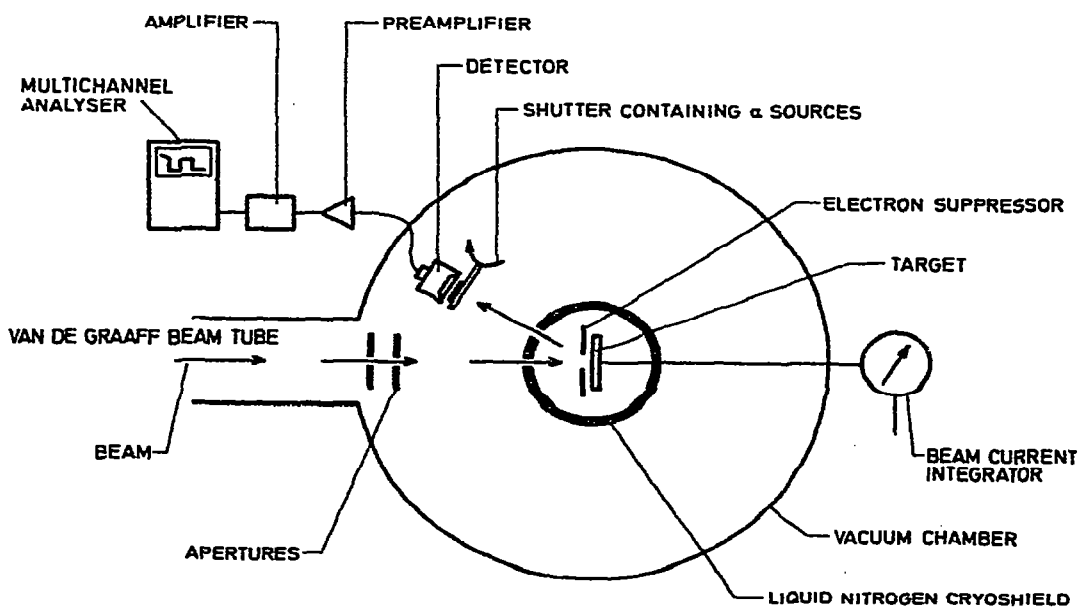


Fig. 3. Schematic diagram of the backscattering arrangement

Samples are mounted in a vacuum chamber which is connected to the beam tube of a Van de Graaff accelerator. Vacuum requirements are not stringent with  $10^{-5}$  -  $10^{-6}$  mbar normally found to be adequate. The accelerator provides a monoenergetic beam of ions which impinge on the sample. The energetic particles back-

scattered through a fixed laboratory angle are detected by a surface barrier detector. The energy of the scattered projectile,  $E$ , is always less than the incoming energy  $E_0$  and is given by  $E = KE_0$ , where  $K$  is the kinematic factor of the collision. This can be calculated from the classical conservation laws of energy and momentum. It can be shown that  $K$  is a function only of the mass of the projectile  $M_p$ , the mass of the target atom  $M_T$  and the scattered angle of the projectile  $\theta_s$ . For the extreme case of the projectile being scattered through  $180^\circ$ ,  $K$  reduces to:

$$K = \left( \frac{M_T - M_p}{M_T + M_p} \right)^2 \quad (3)$$

This illustrates the fact that RBS is able to discriminate between the different elements making up a target.

A typical backscattering spectrum is shown in Fig. 4. The target material was silicon implanted with bismuth, with a thin layer of copper ( $7.87 \mu\text{g cm}^{-2}$ ) evaporated on the silicon surface. The sample was bombarded with helium ions at an energy of 2 MeV. Fig. 4 shows sharp and well separated peaks due to the Cu and Bi. From the peak areas  $A_{\text{Cu}}$  and  $A_{\text{Bi}}$ , the scattering cross sections  $\sigma_{\text{Cu}}$

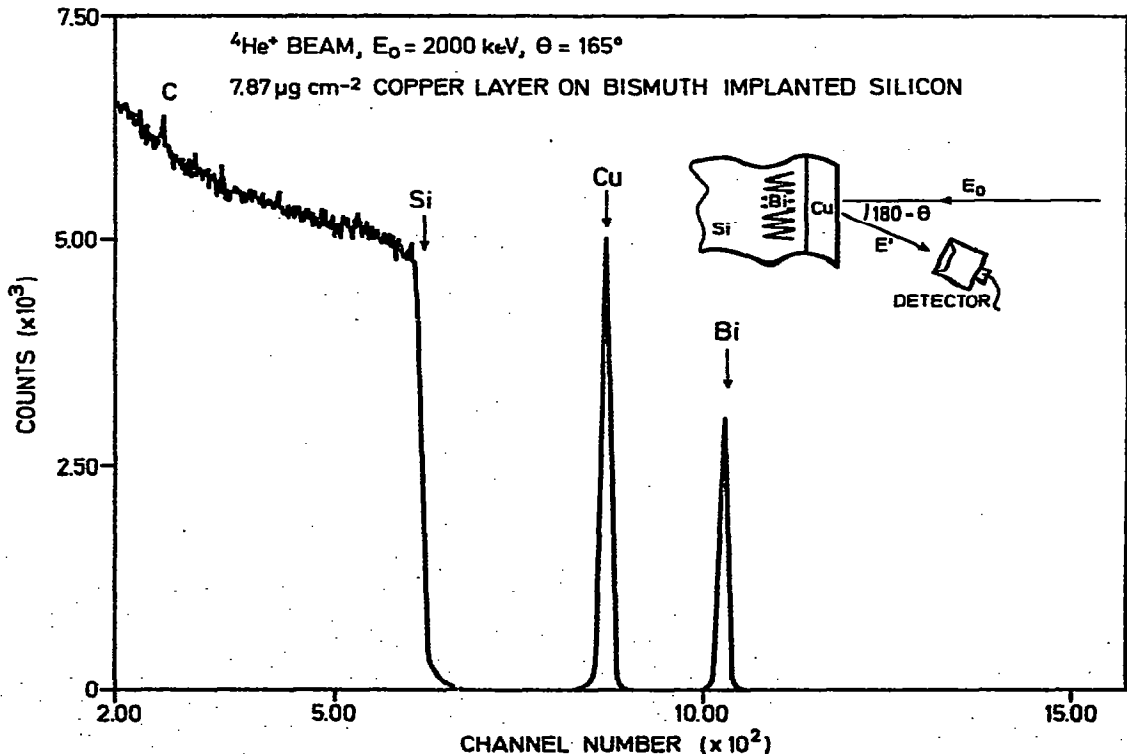


Fig. 4. Backscattering spectrum from copper evaporated on bismuth implanted silicon

and  $\sigma_{\text{Bi}}$  and the known areal density of the copper deposit  $m_{\text{Cu}}$ , the areal density of the bismuth implant  $m_{\text{Bi}}$  (atoms  $\text{cm}^{-2}$ ) can be calculated:

$$m_{\text{Bi}} = \frac{A_{\text{Bi}}}{A_{\text{Cu}}} \frac{\sigma_{\text{Cu}}}{\sigma_{\text{Bi}}} m_{\text{Cu}} \quad (4)$$

The accuracy of the determination of  $m_{\text{Bi}}$  depends directly on the accuracy with which the areal density of the copper layer has been determined.

By making very careful evaporations and weighings of the Cu layer it has been possible to determine the absolute quantity of the bismuth implant to  $4.94 \cdot 10^{15}$  atoms  $\text{cm}^{-2}$  with an uncertainty smaller than 2 % (Ref. 13). This type of ion implanted sample may then be used as a robust reference material of accurately known dose for RBS applications.

Another example, for a composite reference layer, is the following. Some techniques for surface analysis make use of ion bombardment to sputter etch surface layers in order to have access to near-surface regions. For accurate depth profiling proper adjustment of the sputtering parameters is important. This can be achieved by using well defined multi-layers. Such layers have been prepared and weighed in situ. Two examples of multi-layers one on a silicon and the other on a vitreous carbon backing are given schematically in Fig. 5.

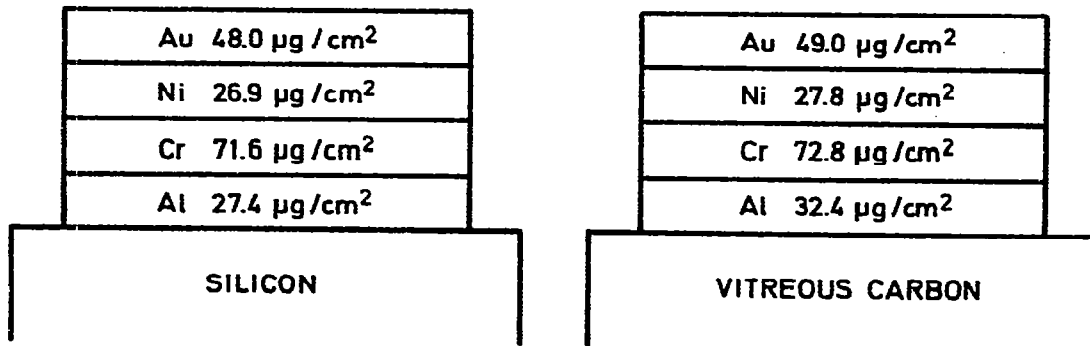


Fig. 5. Multilayers Au/Ni/Cr/Al on silicon and vitreous carbon

The indicated layer thicknesses have been determined by microweighing. The RBS spectra of such layers are shown in Fig. 6. For Au, Ni, and Cr both spectra are identical; in the case of the silicon backing (dashed line) the Al peak overlaps with the Si spectral edge, whereas in the case of vitreous carbon the Al peak is well isolated.

#### Self-supporting foils

In many applications of self-supporting foils it is important to know their areal densities with high accuracy. Examples are: supports for thin backings.



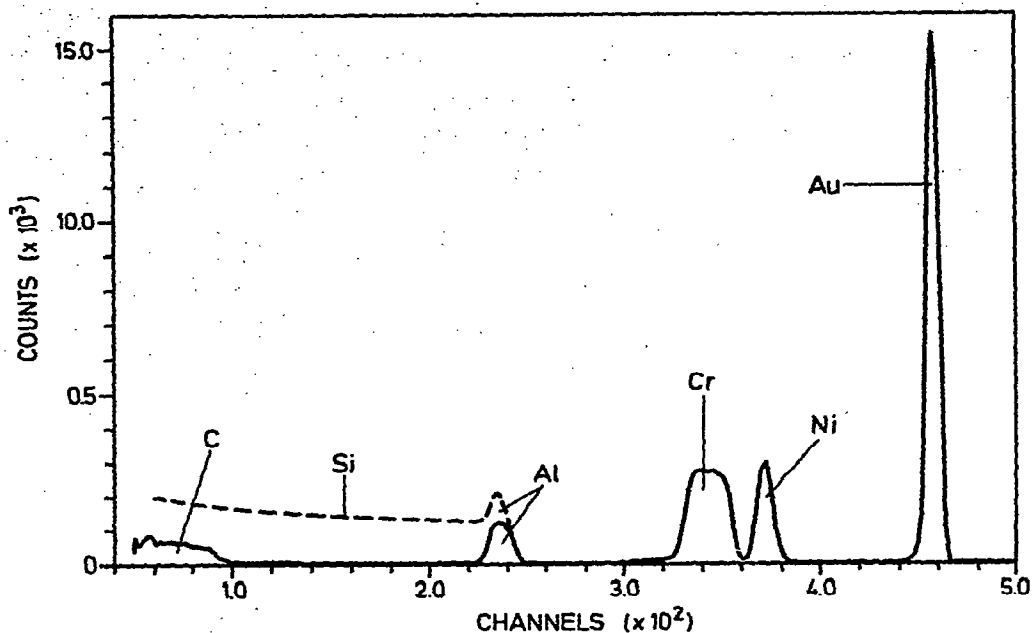


Fig. 6. RBS spectrum of multilayer on silicon and vitreous carbon

used in nuclear measurements, stripper foils, energy filters. The thickness of such foils in the region of several  $\mu\text{g cm}^{-2}$  to several  $\text{mg cm}^{-2}$  can be easily and accurately determined by measuring the energy loss of  $\alpha$ -particles traversing these foils (ref. 14). The experimental arrangement for these measurements is schematically shown in Fig. 7.

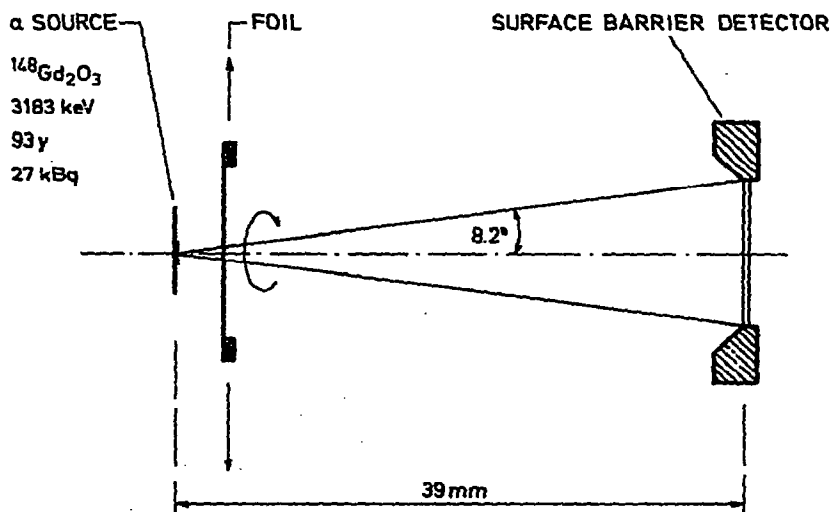


Fig. 7. Foil thickness measurement by  $\alpha$ -absorption

The energy spectrum of a  $^{148}\text{Gd}$   $\alpha$  source is measured by a Si barrier detector with and without inserting a foil between the  $\alpha$  source and detector. From the energy shift towards lower energies of the  $\alpha$  peak, due to the foil, and by applying a modified Gaussian fit (ref. 15) to the measured peaks, sensitivities in areal density of a few tenths of a  $\mu\text{g cm}^{-2}$  can be obtained. However, to employ this simple method to its full capability, calibration foils are needed. For their preparation, highly polished disks of fused silica, with a diameter of 40 mm and a thickness of 0.6 mm, were used as substrates. Prior to the evaporation of the metallic reference films a thin sodium chloride layer ( $30 \mu\text{g cm}^{-2}$ ), to serve as release agent, was deposited from a resistively heated boat. After metallising the final layers were scribed into squares and floated off the silica disk into a basin containing distilled water. The resulting thin reference foils could then be picked up onto standard circular (annuli) holders having holes of 6 mm diameter.

For the preparation of thin carbon foils essentially the same technique was applied. However, after NaCl deposition and weighing, the substrates were transferred to a different vacuum system where the layer was produced by the carbon arc method. For the mass determination, the substrate with the deposited foil was transferred back to the uhv system where, after evacuation, the mass of the carbon deposit was determined by the microbalance. The accuracy of these measurements was checked by applying different methods which included weighing of large foils with an ordinary microbalance at atmospheric pressures. It has been shown that the areal density of carbon foils can be determined with an uncertainty of less than  $2 \mu\text{g cm}^{-2}$ . Finally Fig. 8 shows the energy loss of  $\alpha$  particles versus foil thickness for different materials.

#### CONCLUSION

Since measurements on an uhv microbalance are directly traceable to primary mass standards, weighings with high accuracy are feasible. The microbalance has been extremely useful in a number of applications for the assay of thin standard layers and foils. Together with other analytical methods of comparable sensitivity (e.g. RBS) valuable information on thin composite layers can be obtained.

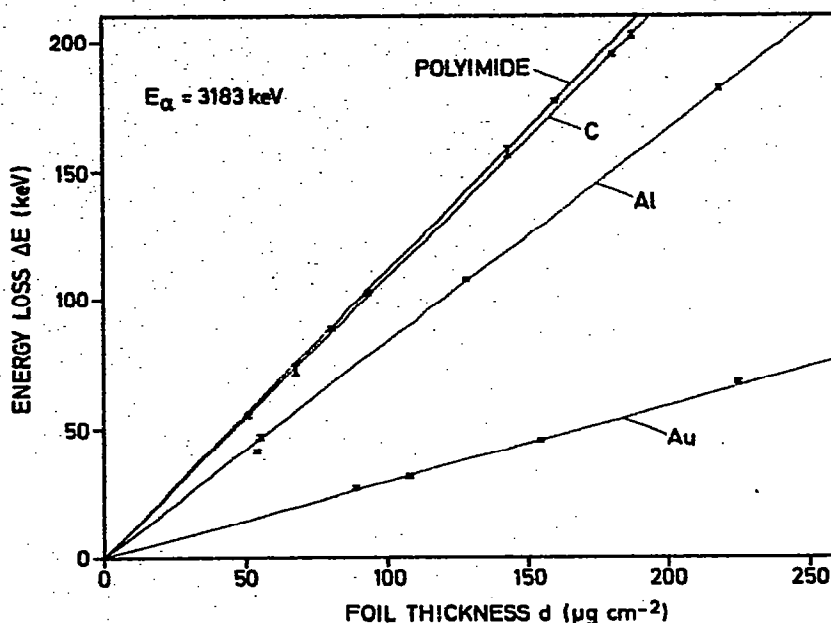


Fig. 8. Energy loss in function of the layer thickness for different materials

#### REFERENCES

- 1 J. Van Audenhove, H.L. Eschbach and H. Moret, Nucl. Instr. Meth. 24 (1963) pp.465-470.
- 2 H. Moret and E. Louwerix, Vacuum Microbalance Techniques, Vol. 5. (1965) pp.59-75.
- 3 H. Moret, E. Louwerix and E. Sattler, Vacuum Microbalance Techniques, Vol. 7. (1970) pp.173-179.
- 4 H.L. Eschbach and A. Grillot, Le Vide N° 140, (1969) pp.97-104.
- 5 H.L. Eschbach, Nucl. Instr. Meth. 102 (1972) pp.469-475.
- 6 H.L. Eschbach and H. Moret, Vakuumtechnik 17 (1968) pp.29-33.
- 7 J. Brulmans, Internal Report CBNM/AS/09/76 (1976).
- 8 W. van der Eijk and H. Moret, Standardization of Radionuclides, I.A.E.A., Vienna (1967) p.529.
- 9 G. Sauerbrey, Z. Phys. 155 (1959) p.206.
- 10 H.L. Eschbach and E.W. Kruidhof, Vacuum Microbalance Techniques, Vol. 5. (1965) pp.207-216.
- 11 L.I. Maissel and R. Glang, Handbook of Thin Film Technology, McGraw Hill, New York (1970).
- 12 B. Ramadan, K. Piyakis and J.F. Kos, Rev. Sci. Instr. 50 (1979) pp.867-871.
- 13 I.V. Mitchell and H.L. Eschbach, Nucl. Instr. Meth. 149 (1978) pp.727-733.
- 14 H.L. Eschbach, R. Werz, I.V. Mitchell and P. Rietveld, Proc. 8th Intern. Vac. Congress, Cannes 1980, Vol. I, Thin Films, pp.267-270.
- 15 R. Werz and I.V. Mitchell, Internal Report CBNM/MS/1/80 (1980).